Influence of Process Parameters on the Mechanical Properties of the Reformer Tube

Jiahe Zhang [1,*], *Wenjia* Yin[1] , and *Peng* Jiang [2]

[1] Mechanical Science and Engineering College, Northeast Petroleum University, Daqing 163318, Heilongjiang, China
[2] Chemical Fertilizer Plant of Daqing Petrochemical Company, Daqing, Heilongjiang 163714)

Abstract. Considering the non-linear characteristics of the reformer tube material with temperature changes and the influence of the fluid inside and outside the tube, we suggest to establish a thermal-fluid-solid coupling model and calculation method for the reformer tube of the hydrogen production reformer. The multi field coupling theory is used to analyze and study the stress distribution of the fluid in the reformer tube under different process conditions, different inlet temperature and different inlet flow rate.We found that under hot operating conditions, as the fluid inlet temperature in the tube increasing, the maximum equivalent stress of the overall reformer tube structure gradually decreased. As the flow rate gradually increasing, the maximum equivalent stress of the reformer tube decreased gradually and then increased. In this paper, all the technological parameters come from the actual production conditions, so the research results provide a certain reference for safe production.

1 Introduction

Hydrogen production by natural gas steam reforming has been used in the industrial field since 1926 and now has a history of nearly 100 years. It has the advantages of low cost and convenient operation. It is the most mature and widely used hydrogen production method in the industry[1]. Methane steam reforming reaction is a process of increasing volume. As the pressure increasing, the equipment capacity and the utilization rate of the catalyst have been improved. The pressure of the methane steam reforming reaction in the actual reformer is between 3.0 and 4.0MPa. At the same time, the methane steam reforming reaction is a strong endothermic reaction and the increase of the reaction temperature is conducive to improving the methane conversion rate[2]. However, the reaction temperature must be limited by the heat resistance of the conversion tube material. Therefore, the appropriate airspeed index should be selected in actual production. The airspeed is generally controlled between $650h^{-1}$ and $1000h^{-1}$ in China and between$1300h^{-1}$and$2000h^{-1}$ in foreign countries[3]. Many scholars at home and abroad have studied the reaction of methane steam reforming and multi-field coupling mechanical analysis. Murphy DM[4] studied the heat transfer, flow and reaction kinetics of methane steam reforming in a ceramic microchannel reactor, Liu Jubao et al[5] used a domain coupling method to analyze the double-layer tube and the fluid inside and outside the tube. A multi-field coupling simulation was carried out and a distributed collaborative solution method was proposed to solve the multi-field coupling problem.

There are few studies on the influence of the fluid inside and outside the tube on the stress of the reformer tube under the operating conditions of the reformer tube in previous studies. Considering the influence of the fluid inside and outside the reformer tube on the reformer tube, this paper takes the reformer tube as the research object under the actual working conditions of a hydrogen production reformer. The multi-field coupling mechanical analysis is carried out. The mechanical properties of the reformer tube under the influence of different inlet temperature and inlet velocity of fluid in the reformer tube are investigated under the thermal operating condition. It is expected to provide a certain reference for actually safe production.

2 Physical model

The reformer tube of the hydrogen reformer includes an upper pigtail tube, a flange, a reforming tube and other structures. The conversion tube structure is composed of the upper, middle, lower and reduced diameter tubes of the conversion tube. The middle part of the conversion tube is completely located in the radiation chamber and the tube is filled with catalyst particles. The upper part of the tube, the lower part of the tube and the reduced diameter tube are distributed outside the radiant room. The upper section L1 is 162mm long, the middle section L2 is 13000mm long and the lower section L3 is 98mm long. The reformer tube specification is ID110×12. The lower section of the conversion tube is connected to the reduced diameter tube. The reduced diameter tube specification is ID110×ID35, L=145mm. The structure is shown in Figure 1. The material of the upper pigtail tube

* Corresponding author : zjh_nepu@126.com.

and flange structure of the reformer tube is stainless steel TP321H and the structural material of the conversion tube is heat-resistant cast steel ZG40Ni35Cr25Nb. The reformer tubes are suspended by spring hangers and each upper pigtail tube is hoisted with a hanging load of 52N. Each set of reformer tubes are lifted by pulley blocks, the counterweight of the hammer on each reformer tube is 6845N and the reformer tube's own weight is 5237N. Under hot operating conditions, the temperature load on the outer wall of the reformer tube is shown in Figure 2.

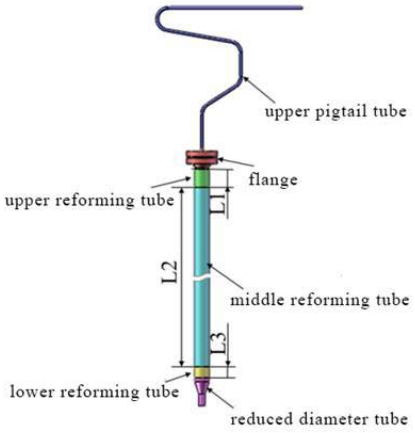

Fig. 1. Schematic diagram of reformer tube.

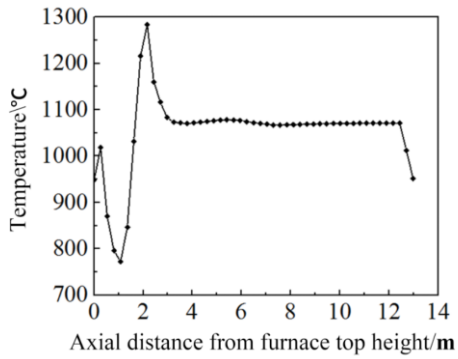

Fig. 2. Temperature load on the outer wall of the reformer tube under hot operating conditions.

3 Establishment of fluid-solid coupling numerical model

3.1 Numerical model of fluid-solid coupling

Taking the fluid in the middle section of the conversion tube as the research object, using a spatial eight-node hexahedral element, the finite element model of the reformer tube fluid domain is established as shown in Figure 3. The inlet velocity boundary Vin is 1m/s and the inlet temperature Tin is 520℃.The outlet pressure boundary Pout is 3.01Mpa and the outlet temperature Tout is 850℃. Considering the uneven temperature of the fluid in the radiation chamber outside the tube, the wall temperature of the reformer tube fluid area is the variable temperature load at the position of the reformer tube calculated by the fluid in the radiation chamber. Taking the overall structure of the reformer tube as the research object, the finite element model of the reformer tube solid domain is established as shown in Figure 4. The reformer tube is hoisted by a pulley block. Considering the weight of the reformer tube, full constraints are imposed on the upper tube end of the upper pigtail tube and the lower tube end of the conversion tube.

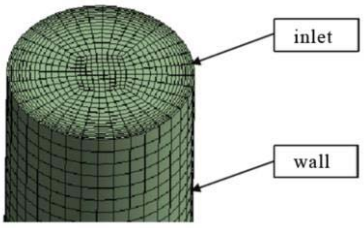

Fig. 3. The finite element model of the reformer tube fluid domain.

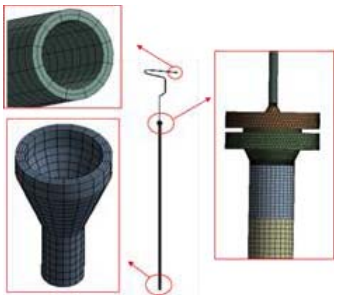

Fig. 4. The finite element model of the reformer tube solid domain.

3.2 Fluid-solid coupling Fluid-solid coupling calculation method

When finite element method is used to solve the fluid-solid coupling problem of reformer tube, the fluid domain and the solid domain should be discretized by finite element method. In the process of unit composition, its boundary conditions require forced implementation. According to the different physical domains of nodes, the simplified coupling equation is [6]:

$$\begin{bmatrix} \boldsymbol{A}_{II}^{f} & \boldsymbol{A}_{IC}^{f} & 0 \\ \boldsymbol{A}_{CI}^{f} & \boldsymbol{A}_{CC}^{f}+\boldsymbol{A}_{CC}^{s} & \boldsymbol{A}_{CI}^{s} \\ 0 & \boldsymbol{A}_{IC}^{s} & \boldsymbol{A}_{II}^{s} \end{bmatrix} \begin{Bmatrix} \Delta \boldsymbol{X}_{I}^{f} \\ \Delta \boldsymbol{X}_{C}^{fs} \\ \Delta \boldsymbol{X}_{I}^{s} \end{Bmatrix} = \begin{Bmatrix} \boldsymbol{R}_{I}^{f} \\ \boldsymbol{R}_{C}^{fs} \\ \boldsymbol{R}_{I}^{s} \end{Bmatrix} \quad (3\text{-}1)$$

In the formula, the superscripts f and s are the fluid domain and the solid domain respectively, the subscripts I and C are the variables on the internal nodes and coupling interfaces of the physical domain, $\Delta\mathbf{X}_I^f$ $\Delta\mathbf{X}_C^{fs}$ $\Delta\mathbf{X}_I^s$ are the unknowns of the nodes in the fluid domain and coupling interface, $\boldsymbol{A}^f$ and $\boldsymbol{A}^s$ solid domain respectively Vectors, $\boldsymbol{R}_I^f$ $\boldsymbol{R}_C^{fs}$ $\boldsymbol{R}_I^s$ are the external force vectors of the fluid domain, the coupling interface and the solid domain respectively. In this paper, the structure and interface joint solution method (WC_S) is used to solve the multi-field coupling problem between the reformer tube and the fluid in the tube. Coupling interface is used to be basic boundary and natural boundary in solving fluid domain and solid domain respectively.The internal fluid variables are eliminated to

solve the reformer tube structure by combining the interface. The solution steps are as follows:

1)Solving the fluid domain, according to formula (2-1), we can get:

$$\Delta \boldsymbol{X}_I^f = \left[\boldsymbol{A}_{II}^f\right]^{-1}\left[\boldsymbol{R}_I^f - \boldsymbol{A}_{IC}^f \Delta \boldsymbol{X}_C^{fs}\right] \tag{3-2}$$

Suppose $\Delta \boldsymbol{X}_C^{fs} = 0$, get: $\boldsymbol{A}_{II}^f \Delta \boldsymbol{X}_I^f = \boldsymbol{R}_I^f$ (3-3)

definition: $\boldsymbol{A}_{add}^f = \boldsymbol{A}_{CC}^f - \boldsymbol{A}_{CI}^f\left[\boldsymbol{A}_{II}^f\right]^{-1}\boldsymbol{A}_{IC}^f$ (3-4)

$$\boldsymbol{A}_{add}^f = \boldsymbol{A}_{CC}^f - \boldsymbol{A}_{CI}^f\left[\boldsymbol{A}_{II}^f\right]^{-1}\boldsymbol{A}_{IC}^f \tag{3-5}$$

$$\boldsymbol{R}_{fC}^{fs} = \boldsymbol{R}_C^{fs} - \boldsymbol{R}_{add}^f \tag{3-6}$$

In the formula, considering the correction of the fluid internal force element, $\boldsymbol{A}_{add}^f$ is the additional fluid mass matrix, $\boldsymbol{R}_{add}^f$ is the additional fluid external force vector and $\boldsymbol{R}_{fC}^{fs}$ is the updated margin external force vector.

2) According to the $\boldsymbol{X}_I^f$ updated fluid elements, the updated fluid external force vector $\boldsymbol{R}_{add}^f$ and additional fluid mass matrix $\boldsymbol{A}_{add}^f$ acting on the coupling are transferred to the structure.

3) The solid domain is solved by coupling the interface, according to formula (3-1), formulas (3-7) and (3-8).

$$\left[\boldsymbol{A}_{CC}^f - \boldsymbol{A}_{CI}^f\left[\boldsymbol{A}_{II}^f\right]^{-1}\boldsymbol{A}_{IC}^f + \boldsymbol{A}_{CC}^s\right]\Delta \boldsymbol{X}_C^{fs} + \boldsymbol{A}_{CI}^s \Delta \boldsymbol{X}_I^s = \boldsymbol{R}_C^{fs} - \boldsymbol{A}_{CI}^f\left[\boldsymbol{A}_{II}^f\right]^{-1}\boldsymbol{R}_I^f \tag{3-7}$$

$$\boldsymbol{A}_{IC}^s \Delta \boldsymbol{X}_C^{fs} + \boldsymbol{A}_{II}^s \Delta \boldsymbol{X}_I^s = \boldsymbol{R}_I^s \tag{3-8}$$

According to formula (3-4), formula (3-5) and formula (3-6), formula (3-7) can be abbreviated as:

$$\left[\boldsymbol{A}_{add}^f + \boldsymbol{A}_{CC}^s\right]\Delta \boldsymbol{X}_C^{fs} + \boldsymbol{A}_{CI}^s \Delta \boldsymbol{X}_I^s = \boldsymbol{R}_{fC}^{fs} \tag{3-9}$$

Taking the additional fluid mass matrix, from equation (3-9):

$$\boldsymbol{A}_{CC}^s \Delta \boldsymbol{X}_C^{fs} + \boldsymbol{A}_{CI}^s \Delta \boldsymbol{X}_I^s = \boldsymbol{R}_{fC}^{fs} \tag{3-10}$$

4 Calculation results and analysis

In order to explore the influence of the process parameters of the fluid medium in the tube on the multi-field coupling effect, the multi-field coupling mechanical analysis of the reformer tube is carried out from the inlet temperature and the inlet flow rate to study its influence on the mechanical properties of the reformer tube.

4.1 The influence of inlet temperature on the mechanical properties of reformer tubes

Five inlet temperatures within the normal thermal operating range are selected: 420°C, 470°C, 520°C, 570°C and 620°C. The multi-field coupling mechanics analysis of the reformer tube structure is carried out and the curves of the inlet and outlet pressure difference and the temperature difference of the fluid-solid coupling surface of the reformer tube with the inlet temperature are obtained, as shown in Figure 5 and Figure 6 respectively. The maximum change curve of total displacement of reformer tube structure at different inlet temperatures is shown in Figure 7, the equivalent stress cloud diagram of the overall structure of the reformer tube is shown in Figure 8 and the maximum change curve of the equivalent stress of the reformer tube structure is shown in Figure 9.

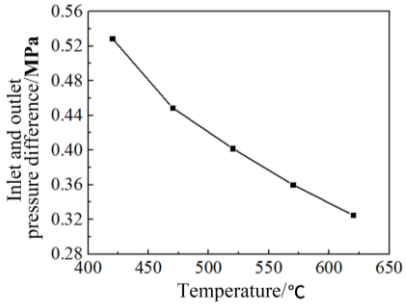

Fig. 5 .Pressure difference between inlet and outlet of fluid-solid coupling surface varies with inlet temperature.

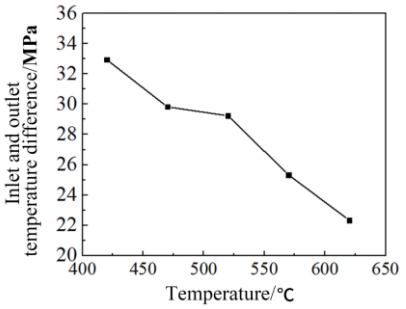

Fig. 6 .The inlet and outlet temperature difference of the fluid-solid coupling surface changes with the inlet temperature.

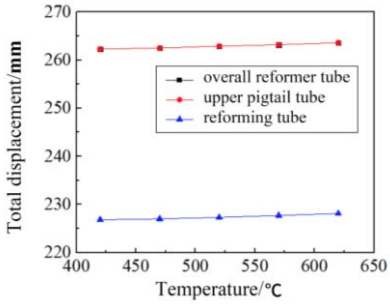

Fig. 7. The maximum total displacement of the reformer tube structure varies with the inlet temperature.

It can be seen from Figure 5 and Figure 6 that with the increase of the reaction gas inlet temperature of the reformer tube, the pressure difference between the inlet and outlet of the fluid-solid coupling surface of the reformer tube decreases from 0.53 MPa to 0.33MPa.It shows a decreasing trend with a rate of 37.74%.The outlet temperature difference drops from 32.95°C to 22.33°C, showing a gradually decreasing trend with a drop of 32.23%. It can be seen from Figure 7 that the maximum total displacement of the overall reformer tube structure appears at the upper pigtail tube. The maximum total displacement of the reformer tube and the upper pigtail tube structure have the same change curve with the inlet temperature. They show a slightly increasing trend from 262.3mm to 263.6mm with an increase of 0.50%.The maximum total displacement of the conversion tube structure increases from 226.8mm to

228.1mm, showing a slightly increasing trend with an increase of 0.57%.

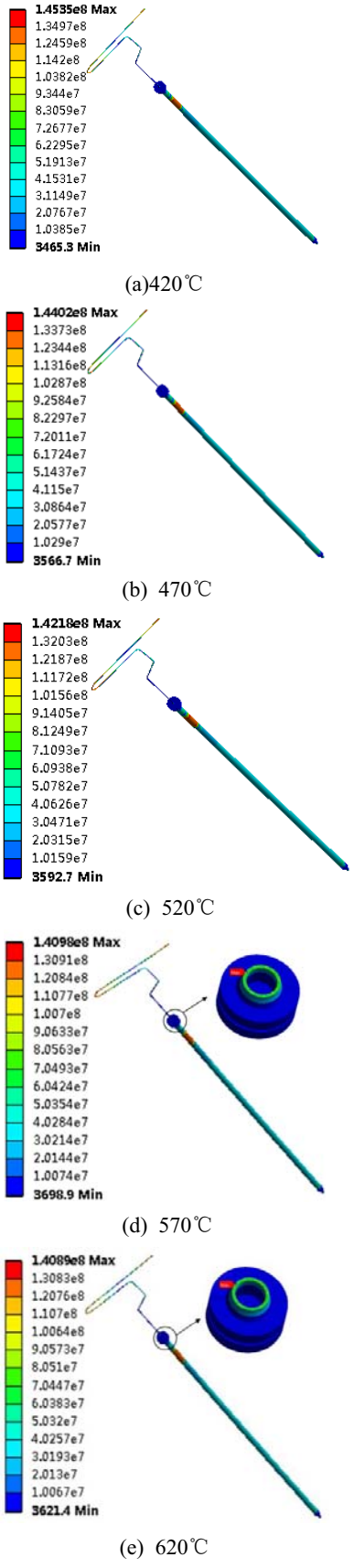

Fig. 8. Equivalent stress cloud diagram of the overall structure of the reformer tube at different inlet temperatures.

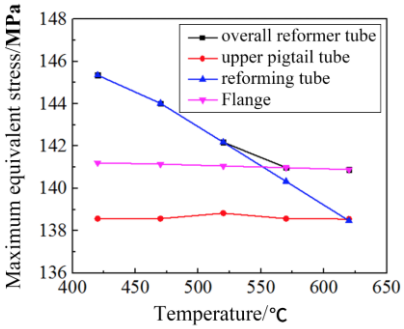

Fig. 9. The maximum equivalent stress of the reformer tube structure varies with the inlet temperature.

It can be seen from Figure 8 and Figure 9 that as the reaction gas inlet temperature of the reformer tube increasing, when the inlet temperature is 420℃~520℃, the maximum equivalent stress of the overall structure of the reformer tube appears on the outer wall of the middle section of the reformer tube. It drops from 145.35MPa to 142.18MPa and shows a gradually decreasing trend with a rate of 2.18%.When the inlet temperature is 570℃ ~620℃, the maximum equivalent stress of the overall structure of the reformer tube appears at the interface between the flange and the conversion tube. It drops from 140.98MPa to 140.89MPa and shows a slightly decreasing trend with a rate of 0.06%. The maximum equivalent stress of the conversion tube structure decreases from 145.35MPa to 138.47MPa and shows a gradually decreasing trend with a rate of 4.73%. The maximum equivalent stress of the upper pigtail tube structure is 138.57MPa and maintains a basically unchanged trend. The maximum equivalent stress of the flange structure decreases from 141.21 to 140.89Mpa and shows a slightly decreasing trend with a rate of 0.23%. The maximum equivalent stress of the flange structure decreases from 141.21 to 140.89Mpa.

4.2 The influence of the inlet flow rate on the mechanical properties of the reformer tube

The influence of different inlet velocities on the mechanical characteristics of reformer tube multi-field coupling under hot operating conditions is studied. Five inlet velocities within the normal thermal operating range are selected: 1.0m/s, 1.5m/s, 2.0m/s, 2.5m/s and 3.0m/s. Through the multi-field coupling mechanical analysis of the reformer tube structure, the curves of inlet and outlet pressure difference and inlet and outlet temperature difference with inlet velocity are obtained, as shown in Figure 10 and Figure 11 respectively. The maximum displacement curve of reformer tube structure under different inlet velocity is shown in Figure 12, the equivalent stress cloud diagram of the overall structure of the reformer tube is shown in Figure 13 and the maximum change curve of the equivalent stress of the reformer tube structure is shown in Figure 14.

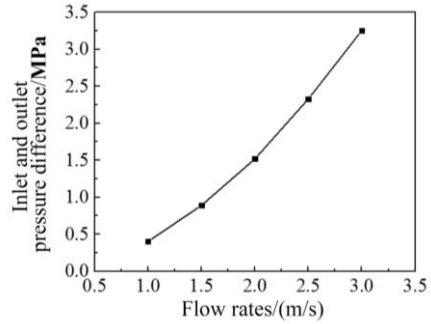

Fig. 10. The pressure difference between the inlet and outlet of the fluid-solid coupling surface varies with the inlet velocity.

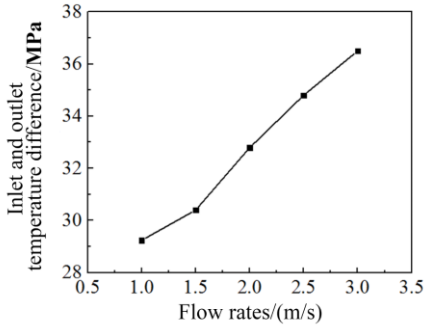

Fig. 11. The temperature difference between the inlet and outlet of the fluid-solid coupling surface varies with the inlet velocity.

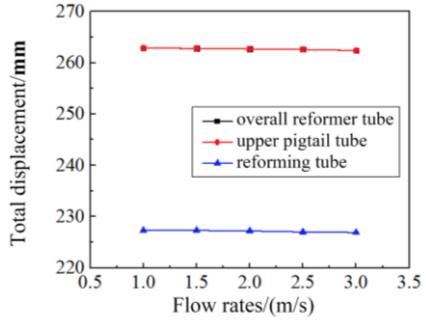

Fig. 12 . The maximum total displacement of the reformer tube structure varies with the inlet velocity.

It can be seen from Figure 10 and Figure 11 that with the increase of the inlet flow rate of the reactant gas in the reformer tube, the pressure difference between the inlet and outlet of the fluid-solid coupling surface of the reformer tube increases from 0.40 MPa to 3.25 MPa and shows a clearly increasing trend with an increase of 7.13 times. The temperature difference between the inlet and outlet of the fluid-solid coupling surface of the reformer tube obviously increases from 29.24℃ to 36.50℃, with an increase of 24.83%. Figure 12 shows that the maximum total displacement of the overall structure of the reformer tube appears at the upper pigtail tube. The maximum total displacement of the overall reformer tube and the upper pigtail structure have the same change curve with the inlet flow rate. They show a slightly decreasing trend from 262.9mm to 262.4mm with a drop of 0.19%. The maximum total displacement of the conversion tube structure decreases from 227.3mm to 226.9mm and shows a slightly decreasing trend with a drop of 0.18%.

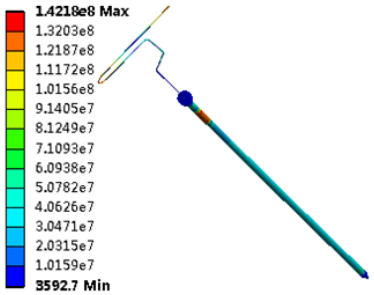

(a)1m/s

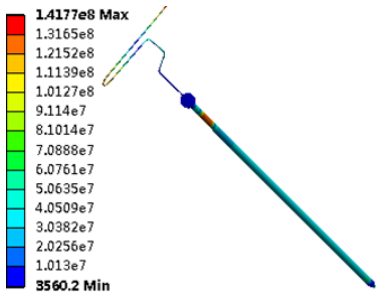

(b) 1.5m/s

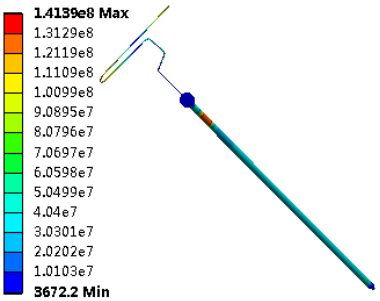

(c) 2m/s

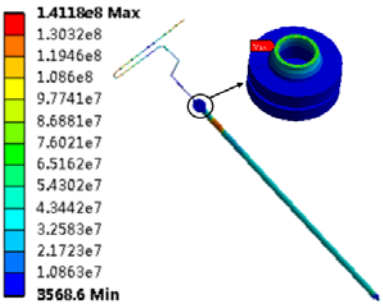

(d) 2.5m/s

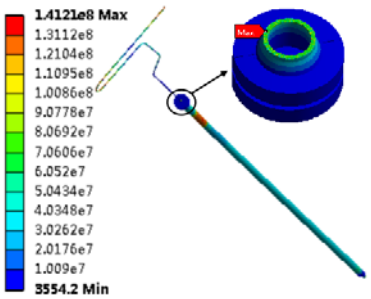

(e) 3m/s

Fig. 13. Equivalent stress cloud diagram of the overall structure of the reformer tube with different inlet flow rates.

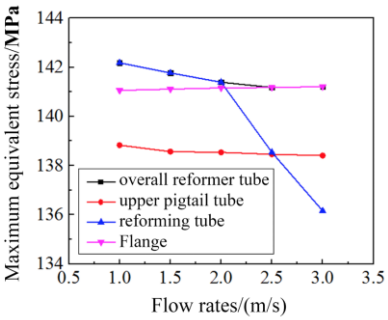

Fig. 14. The maximum equivalent stress of the reformer tube structure varies with the inlet flow rate.

It can be seen from Figure 13 and Figure 14 that under the trend of increasing inlet velocity of reaction gas in the converter tube, when the inlet flow rate is 1m/s~2 m/s, the maximum equivalent stress of the overall structure of the reformer tube appears on the outer wall of the middle section of the reformer tube from 142.18MPa to 141.39MPa .There is a slightly decreasing trend with a drop of 0.56%.When the flow velocity is 2.5m/s~3m/s, the maximum equivalent stress of the overall structure of the reformer tube appears in the flange and transformation. It increases from 142.18 MPa to 141.21 MPa and shows a slightly increasing trend with a rate of 0.02% at the pipe joint. The maximum equivalent stress of the conversion tube structure decreases from 142.18MPa to 136.16MPa and shows a gradually decreasing trend with a rate of 4.23%.The maximum equivalent stress of the upper pigtail tube structure decreases from 138.83MPa to 138.41MPa and shows a slightly decreasing trend with a rate of 0.30%.The maximum equivalent stress of the flange structure decreases from 141.06 to 141.21MPa and shows a slightly increasing trend with a rate of 0.11%.

Fund Project: Project supported by the National Natural Science Foundation of China (51674088); Basic Research Funds for Undergraduate Universities in Heilongjiang Province in 2020, Northeast Petroleum University Guiding Innovation Fund Project (2020YDL-14)

5 Conclusions

1. The influence of different inlet temperatures on the mechanical properties of reformer tube multi-field coupling under hot operating conditions is studied. It is concluded that the maximum total displacement of the overall structure of the reformer tube is located at the upper pigtail tube with the increase of the inlet temperature and shows a slightly increasing trend. When the inlet temperature is 420℃~520℃, the maximum equivalent stress of the overall structure of the reformer tube appears on the outer wall of the middle section of the conversion tube and shows a gradually decreasing trend. When the inlet temperature is 570℃~620℃, the maximum equivalent stress occurs at the joint between the flange and the conversion pipe and shows a slightly decreasing trend.

2. Under hot operating conditions, the influence of different inlet flow rates on the mechanical characteristics of the reformer tube multi-field coupling is studied. It is concluded that with the increase of the inlet flow rate, the maximum total displacement of the overall structure of the reformer tube is located at the upper pigtail tube with a slightly decreasing trend. When the inlet velocity is 1~2m/s, the maximum equivalent stress of the whole reformer tube is located at the outer wall of the middle section of the converter tube and shows a gradually decreasing trend. When the inlet flow velocity is 2.5~3m/s, the maximum equivalent stress is located at the interface between the flange and the conversion tube and shows a slightly increasing trend.

3. Compared with the inlet flow rate factor, the inlet temperature has a strong influence on the multi-field coupling mechanical characteristics of the reformer tube. Therefore, under the hot operating conditions, the stress of the converter tube is mainly caused by temperature and the temperature difference between the inner and outer walls of the tube is the main cause of stress. As the fluid inlet temperature in the tube increasing, the temperature difference between the inner and outer walls of the reformer tube and the maximum equivalent stress of the reformer tube structure decreases accordingly.

References

1. Yushu Z, *Study on the performance of Ni-based catalysts for methane steam reforming in SOFC system*, Harbin Institute of Technology (2019)
2. Changchun S, *Methane-steam reforming hydrogen production reaction and analysis of its influencing factors*, Contemporary Research in Chemical Industry. (5), 62-63 (2019)
3. Murphy DM, Manerbino A, Parker M et al, *Methane steam reforming in a novel ceramic microchannel reactor*. International Journal of Hydrogen Energy. **38**(21), 8741-8750 (2013)
4. Xingying L, Jinsen G, Chunming X et al, *Establishment of a comprehensive numerical simulation mathematical model for the transfer and reaction process in the ethylene cracking furnace*, Acta Petrolei Sinica. **19**(5), 80-85 (2003)
5. Jubao L, Qiang Z, Min L et al, *Numerical simulation of multi-field coupling of double-layer pipe and fluid*, Journal of Daqing Petroleum Institute. **5**(34), 114-121 (2010)
6. Ruojun Q, Shilin D, Xingfei Y, *Research progress of fluid-structure coupling theory*, Space Structure. **14**(01), 3-15 (2008)